Journal of the European Ceramic Society 20 (2000) 1645–1651

A basic gunning material interfaces study

M. Rivenet [a,*], N. Ruchaud [b], J.C. Boivin [a], F. Abraham [a], P. Hubert [b]

[a] *Laboratoire de Cristallochimie et Physicochimie du Solide, ENSCL, BP108, 59652 Villeneuve d'Ascq cedex, France*
[b] *TRB, Unshaped and Pre-cast Refractories Manufacturer, Nesles, 62152 Neufchâtel-Hardelot, France*

Received 15 July 1999; received in revised form 2 November 1999; accepted 6 November 1999

Abstract

Corrosion mechanisms of various basic gunning materials were investigated using crucible tests. The low corrosion resistance of olivine-containing materials was shown to be related to melted phases formation which occurs, at the gunning material/slag interface, at high temperature. MgO-rich materials are more resistant to basic slag attack. Moreover, increasing the refractory material CaO content by means of dolomite addition rises the slag penetration resistance and lowers the bulk modification resulting from slag interaction. In these materials, the corrosion mechanism involves a slag reaction with the starting binder, $(NaPO_3)_n$, and dolomite initially contained in the gunning material. A dolomite-containing material was projected on slag-covered MgO-C bricks, using a laboratory test equipment. Investigations carried out at the gunned material/slag/bricks interface show that the suitable silicophosphate bond still forms, at interface, despite slag interaction.

Keywords: Corrosion; Gunning materials; MgO; Refractories; Slag reactions

1. Introduction

Gunning materials are unshaped refractories commonly used in steel industry for the maintenance of converter linings. Their specific way of processing (projection of a water/powder mixture unto a hot slag-covered wall) (Fig. 1) requires the mixture to have specific rheological properties so as to improve its adherence to the wall.[1,2] Adherence is also reported to be strongly enhanced by slag splashing before gunning.[3] This is usually attributed to slag solidification at interface.[4,5] Moreover, slag splashing after gunning was shown to increase the lifetime of repair.[3] As interaction occurring between the gunning material and slag appears as a major parameter modifying quality of repairing, this work aims to understand the phenomena involved at interface. Crucible tests were carried out using various gunning mixes of well known compositions.[6] The first part of the paper describes the corrosion mechanisms determined on the basis of the X-ray diffraction analyses performed on interfaces. A silicophosphate bonded material mainly made from magnesia and dolomite was found to exhibit the lowest bulk modifications after slag attack. In order to take into account the influence of the gunning process[7,8] on the physical and chemical properties of the interface, this material was sprayed into a rotary furnace in the laboratory. Various analyses methods such as X-ray powder diffraction, X-ray fluorescence, and energy dispersive spectroscopy (EDS) were performed on the gunned material/MgO-C bricks and gunned material/slag/MgO-C bricks interfaces. The results are discussed in the second part of the paper.

2. Experimental

The crucible tests were carried out using the three different types of samples, MC, MDC and MØC, previously studied.[6] All of them were made from calcinated earth-magnesia (M), sodium polyphosphate, and calcium hydroxide (C). In MØC and MDC samples, part of the magnesia was replaced, respectively, by olivine (Ø) or dolomite-clinker (D). An optimum grain distribution was obtained using the theoretical curve of Andreasen[9] with an n exponent equal to 0.35. The crucibles were made, first by mixing the repairing material with 10 wt% of water, then by casting and vibrating the mixtures in $75\times75\times75$ mm^3 moulds. After curing, the crucibles were annealed at 1200°C and filled with an

* Corresponding author.
E-mail address: m.rivenet@ensc.lille.fr (M. Rivenet).

0955-2219/00/$ - see front matter
PII: S0955-2219(00)00024-8

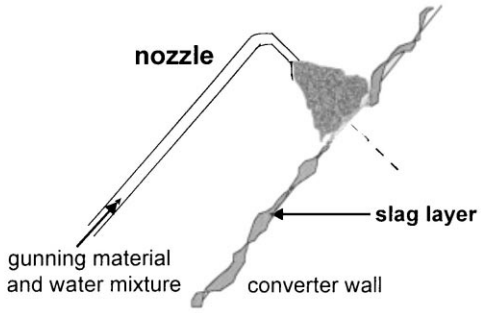

Fig. 1. Schematic diagram of a gunning material projection.

industrial steelmaking slag. The whole was heated at higher temperature (1600°C) for 5 h. The corrosion profile was determined by analysing the diagonal section. The slag/refractory material interface was sampled, ground, and analysed using X-ray powder diffraction.

The gunning experiments were carried out in the laboratory in order to simulate, ideally, the conditions occurring during actual repairs of the converters. The experiments were performed using a smaller gunning device than the one operating on steelplant. This led the proportion of water mixed with the raw material to be adjusted in order to ensure an optimum viscosity of the material. Air pressure was optimised (0.5 bar) with respect to the distance between the nozzle and the linings (10 cm). Owing to the laboratory conditions requirement, a tube brought tap water to the middle of the nozzle (to the beginning on steelplant). During the first experiment, the gunning material was sprayed into a MgO-C bricks lined rotary furnace. During the second experiment, industrial slag was introduced into the furnace prior to the gunning material projection. In both cases, the rotary furnace was heated with an oxypropane flame. The temperature was measured using a pyrometer. Once the furnace cooled down, the coated bricks were longitudinally cut. The gunned layers were sampled along the cross-sections in order to perform X-ray powder diffraction and EDS analyses versus the distance between the sample and the brick surface.

X-ray powder diffraction patterns were recorded at room temperature by means of a Siemens D5000 θ-2θ diffractometer using Bragg–Brentano geometry with a back-monochromated Cu-K_α radiation. The phase identification was performed by means of the PDF data base of the JCPDS using the PC software package diffrac-at of SOCABIM.

For microscopic study, 2 cm^2 areas block samples were mounted in resin, polished and carbon-coated. They were examined in secondary electron imaging mode on a Philips SEM-525M scanning electron microscope. EDS was done using an EDAX PV 9900 system with a Si–Li detector supplied with an ultra-thin window which makes it possible to detect light elements. The results were corrected from matrix effects using the ZAF correction method including atomic number, absorption and fluorescence corrections.

X-ray fluorescence analyses were carried out using a wavelength dispersive SRS300 Siemens spectrometer equipped with a rhodium anode (50 keV, 50 mA), proportional counters (flow and scintillation counters) and a sequential analyser. The samples were prepared using a lithium-based flux.

3. Results and discussion

3.1. Raw materials characterisation

The raw materials have been extensively described elsewhere,[6] so, only their main characteristics are herein described.

The magnesia contains 1.4 wt% of CaO. Its basic index, $\frac{CaO}{SiO_2}$, equal to 0.5, is in agreement with the nature of oxide impurities (Mg_2SiO_4, $CaMgSiO_4$, and $MgAl_2O_4$ spinel phase) present in the samples previously heated at 1200, 1400 and 1600°C.[10] Olivine added to MØC samples contains 7.6 wt% of Fe_2O_3. The dolomite clinker used in MDC materials consists in a mixture of CaO and MgO phases accompanied with Ca_3SiO_5 and $Ca(Fe,Al)_2O_5$ as minor phases. An average of 15 units per chain was found for the bonding Graham salt, $(NaPO_3)_n$. The calcium hydroxide used as a setting agent was shown to also contain some $Ca_{1.5}SiO_{3.5}.xH_2O$.

A slag with a basic index $\frac{CaO}{SiO_2}$ equivalent to 3.72 (Table 1), was sampled from a steelplant converter, at the end of the steel refining process. X-ray diffraction analysis shows that the solid part of this slag, once cooled down, is composed of β-Ca_2SiO_4, FeO and $Ca_{0.9}Mn_{0.10}O$ as major phases and $Ca_2Fe_2O_5$ as a minor phase. In order to increase the iron content, a second slag was made by adding 5 wt% of iron to the previous slag.

3.2. Corrosion tests

3.2.1. Crucibles corrosion profile

The corrosion profiles exhibit various aspects depending upon the crucibles and slag compositions. Whatever the used slag, the olivine-containing MØC samples were highly worn whereas the dolomite-containing MDC samples and the magnesia-based MC materials were less corroded. Interactions between MDC samples and slag has led to a strong interface densification. In MC samples, slag infiltration results in

Table 1
Chemical composition of the steelmaking slag

Oxide	CaO	Fe_2O_3	SiO_2	MgO	MnO	P_2O_5	Al_2O_3	TiO_2	C/S
wt%	51.34	18.98	13.78	7.73	3.00	2.40	2.17	0.60	3.72

two different coloured zones. Corrosion profiles are not modified by increasing the slag iron content, however, infiltration depth in MC samples is increased.

3.2.2. X-ray diffraction analyses

Crystalline composition of the heated samples and interfaces are reported in Table 2. X-ray diffraction patterns of the uncorroded MØC samples evidence the presence of large amounts of MgO and forsterite, Mg_2SiO_4, and of a minor spinel phase. After corrosion, those three phases are still present. Moreover, X-ray diffraction diagrams exhibit monticellite, $CaMgSiO_4$, associated with a decrease of the Mg_2SiO_4 content. An increase of the slag iron content further decreases the proportion of Mg_2SiO_4 remaining in the sample.

The uncorroded MC samples contain large amount of MgO and minor quantities of forsterite, Mg_2SiO_4. Various phosphate phases such as $Na_3Ca_6(PO_4)_5$,[11] $Ca_9MgNa(PO_4)_7$ or $NaCaPO_4$ were also evidenced.[6] Slag penetration involves large modification in the crystalline composition of the samples. Mg_2SiO_4 disappears while the formation of $CaMgSiO_4$ is observed. The phosphate X-ray diffraction pattern evolves in agreement with the formation of a sodium calcium silicophosphate. An additional spinel phase crystallises. A new diffraction peak which could be attributed to a calcium iron oxide occurs at $2\theta = 33.5°$.

Before corrosion, the MDC samples X-ray diffraction patterns evidence, besides MgO, the presence of CaO, $Ca(OH)_2$ and of a calcium sodium silicophosphate solid solution of $Na_{2-x}Ca_{5+x}(PO_4)_{4-x}(SiO_4)_x$ type.[6] Interaction with slag leads to small changes in the X-ray diffraction pattern of the MDC samples. MgO, CaO, $Ca(OH)_2$ and the silicophosphate phase remain present when using slag 1. As for MC samples, a diffraction peak appears at $2\theta = 33.5°$. Only when increasing the slag iron content, CaO disappears. An additional phase which could be $Ca_2MgFe_2O_6$ was evidenced.

3.2.3. Corrosion mechanisms

The corrosion mechanism of MØC samples was determined by means of additional investigations in the $CaO.SiO_2.MgO$ and $MgO.FeO.SiO_2$ diagrams. Bold part of line *a* joining Ca_2SiO_4 and Mg_2SiO_4 in the CaO–SiO_2–MgO diagram (Fig. 2),[12] indicates that a solid solution of monticellite type forms, at high temperature, between those two compounds. Cooling the solid solution leads to $CaMgSiO_4$ crystallisation. Both the $CaMgSiO_4$ appearing and Mg_2SiO_4 content decrease, found at MØC/slag interfaces, were, therefore, attributed to the reaction, at high temperature, between Mg_2SiO_4 and Ca_2SiO_4 respectively brought by the refractory material and slag. The strong wear of crucibles was explained considering the melted phases with compositions ❶ and/or ❷, which occur at 1600°C, when mixing slag and MØC samples (Fig. 2, line b). The higher decrease of Mg_2SiO_4 content observed in presence of a higher iron content shows that Mg_2SiO_4 reacts with iron. The olivine solid solution, $(Mg,Fe)_2SiO_4$, resulting from this reaction, lowers the melting point compared to that of Mg_2SiO_4 (Fig. 3)[13] leading to additional melted phases.

$CaMgSiO_4$ appearing in corroded MC samples was also assumed to result from the reaction between Mg_2SiO_4 and Ca_2SiO_4. However, owing to the lower Mg_2SiO_4 content in MC than in MØC samples, some Ca_2SiO_4 provided by slag remain in excess. Thus, they react with the phosphorus contained in the crucibles leading to the evidenced silicophosphate. The spinel phase crystallisation was probably originated from the periclase dissolution in slag.

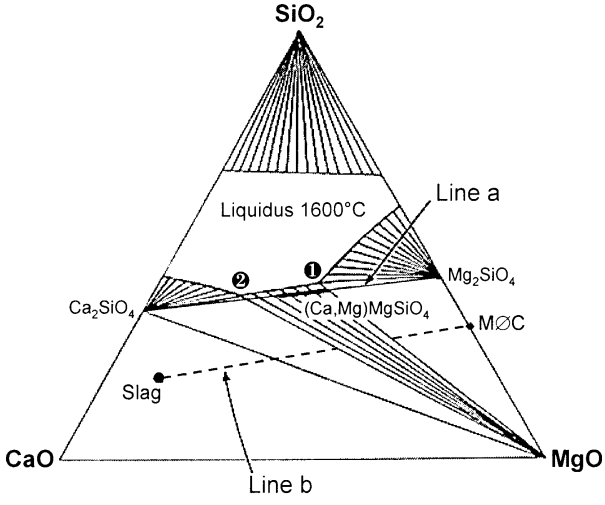

Fig. 2. MgO–CaO–SiO_2 diagram[12] redrawn at 1600°C.

Table 2
Comparison of the crystalline composition of the basic gunning materials before and after corrosion

Gunning material	Crystalline composition	
	After heating at 1600°C[6]	After interacting with slag
MØC	MgO, Mg_2SiO_4, small amount of spinel phase	MgO, Mg_2SiO_4, $CaMgSiO_4$, spinel phase
MC	MgO, phosphate phase, small amount of Mg_2SiO_4	MgO, silicophosphate solid solution, spinel phase plus a $2\theta = 33.5°$ reflection (calcium iron oxide)
MDC	MgO, CaO, $Ca(OH)_2$, silicophosphate solid solution	MgO, CaO, $Ca(OH)_2$, silicophosphate solid solution plus a $2\theta = 33.5°$ reflection (calcium iron oxide)

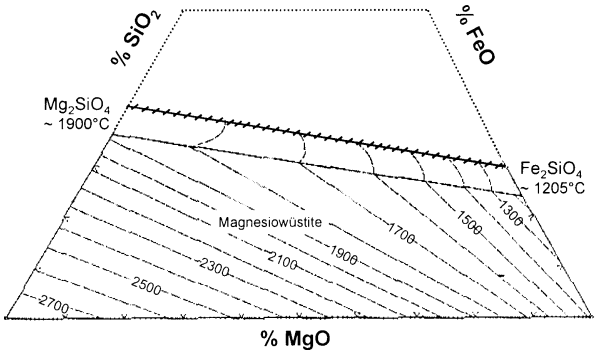

Fig. 3. Part of the ternary diagram MgO–FeO–SiO_2 redrawn from Ref. 13.

The limited slag infiltration in dolomite-containing materials has already been reported in the literature.[14,15] The behaviour of MDC materials in presence of slag was found in agreement with the previous studies. Moreover, the present work shows that the modifications of the MDC materials crystalline composition which results from slag penetration, are very low. This material was chosen to be projected into the rotary furnace. First, the gunning material was projected on bricks, without slag, in order to investigate the effects of projection and temperature gradient on the characteristics of the gunning material. Then, the gunning material/slag/bricks interface was examined.

3.3. The gunned material

3.3.1. Gunning operation and temperature effects

The first gunning experiment was carried out by spraying the gunning material directly unto MgO-C bricks. Temperature evolution during the experiment is reported on Fig. 4. The furnace was, first heated at 1600°C. Owing to the temperature decreasing from 1600 down to 900°C during gunning operation, the furnace was re-heated to 1600°C and, then, hold at this temperature for half an hour.

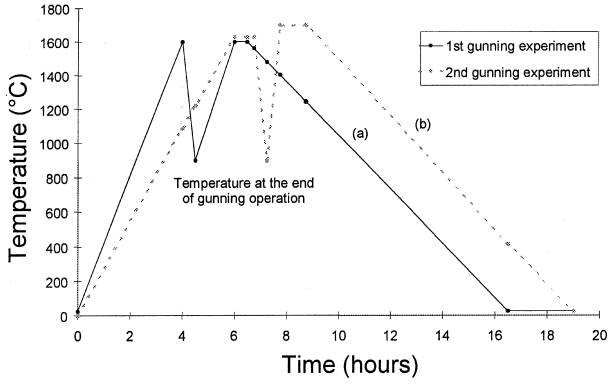

Fig. 4. Temperature measurements during the (a) first and (b) second gunning experiments.

The gunning operation yields a lower density (1865 $kg\,m^{-3}$) and a higher porosity (35%) than that of a moulded material heated at the same temperature (2258 $kg\,m^{-3}$, 25%).

X-ray fluorescence analyses evidenced that the chemical composition of the gunned material varies along the longitudinal section. Particularly, its Na_2O and P_2O_5 contents increase from hot face to cold face. At interface, the Na_2O and P_2O_5 proportions are higher than those initially present in MDC materials (Fig. 5). This was related to the binder migration from hot face to cold face. Such an effect of the temperature gradient was previously reported for Na_2SiO_3 bonded gunning materials[16] but was, to our knowledge, never evidenced, in ($NaPO_3$)-containing materials.

X-ray diffraction analyses of the internal layers evidenced the presence of $NaCaPO_4$ and $Ca_5(PO_4)_3OH$ whereas the silicophosphate phase was observed at hot face. $NaCaPO_4$ and $Ca_5(PO_4)_3OH$ are the low temperature forms of a precursor of the silicophosphate bond.[6,17] Their presence indicates that the corresponding layers were heated at a temperature lower than 1100°C.

The composition and texture of the bond was also found to strongly evolve along the cross section of the gunned sample (Fig. 6). At MDC/MgO-C interface, the bond surrounds rounded MgO crystals and exhibits pores. It contains large amounts of sodium and phosphorus. The presence of rounded MgO crystals well coated by the rich Na and P bonding phase indicates that adhesion of the gunning material to the wall occurs with the aid of a viscous phase [probably melted $(NaPO_3)_n$] which dissolves the biggest grains. As the temperature increases from cold face to hot face, the bonding phase composition and microstructural aspect change. The Na and P contents of the silicophosphate bond are progressively substituted by Ca and Si. This is in agreement with the temperature increase and the resulting reaction of $(NaPO_3)_n$ with the intergranular

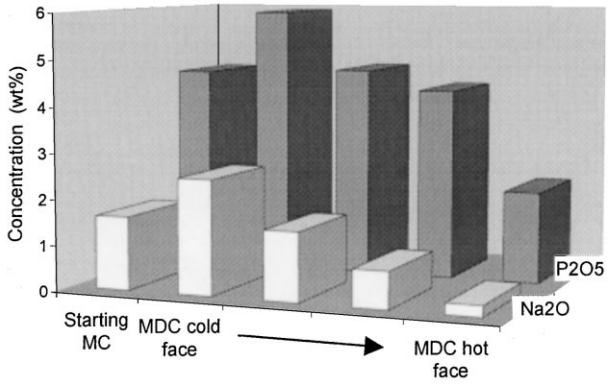

Fig. 5. X-ray fluorescence analyses of Na_2O and P_2O_5, in the gunned MDC, material versus the analysed section: comparison with the Na_2O and P_2O_5 concentrations initially present in MDC.

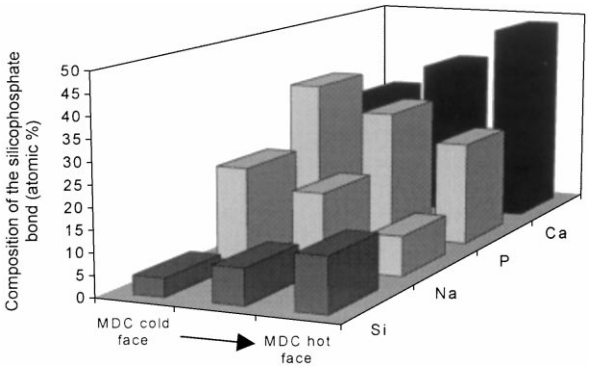

Fig. 6. EDS analyses of the MDC material silicophosphate bond after projection on MgO-C bricks.

silicate phases of the refractory grains.[4,6] The rise of Ca and Si contents improves refractoriness of the bond which now surrounds magnesia and dolomite grains as well as rounded MgO crystals. The sample microstructure and the silicophosphate composition in hot layer (Na/Ca/P/Si = 9.5/48.5/24.5/13) are close to those observed in a moulded MDC material previously heated at 1400°C (Na/Ca/P/Si = 12.7/49.5/18.7/15.6)[6] indicating that this section has, approximately, reached this temperature.

3.3.2. The MDC/MgO-C corroded interface analyses

Temperature evolution during the second experiment is represented in Fig. 4. 2.7 kg of the slag used for crucible test was progressively added into the furnace. Once the MgO-C bricks entirely covered by the melted slag, the furnace was maintained at 1630°C for 45 min. Then, part of the slag was sampled in order to be analysed. Following the temperature decrease occurring during the gunning operation, the furnace was re-heated at about 1700°C for 1 h.

After heating at 1630°C, the crystalline composition of the slag has changed: Ca_2SiO_4 and $Ca_2Fe_2O_5$ were evidenced as major phases, $Ca_{0.9}Mn_{0.10}O$, Ca_3SiO_5 and MgO as minor phases. The two main slag phases, Ca_2SiO_4 and $Ca_2Fe_2O_5$, were evidenced in the X-ray diffraction patterns of slag infiltrated MgO-C bricks. X-ray diffraction patterns of interfacial gunned MDC exhibit the presence of MgO, CaO, $Ca(OH)_2$ and of the silicophosphate phase accompanied with the typical diffraction peak located at $2\theta = 33.5°$. EDS analyses latter confirmed that this peak accounts for an iron calcium oxide.

A schematic profile of the longitudinal section is given Fig. 7. The bricks display large MgO grains. The slag presence was evidenced by a calcium iron oxide, containing some calcium silicate crystals, found in the infiltrated regions. MDC material was identified by means of the (silico)phosphate bonded grains.

In unfiltered bricks (region I), some magnesiowüstite crystals, (Mg,Fe)O, containing about 7% iron and small amounts of silicon (~1.3%) were identified alongside MgO grains. They result from the slag and MgO grains interaction.

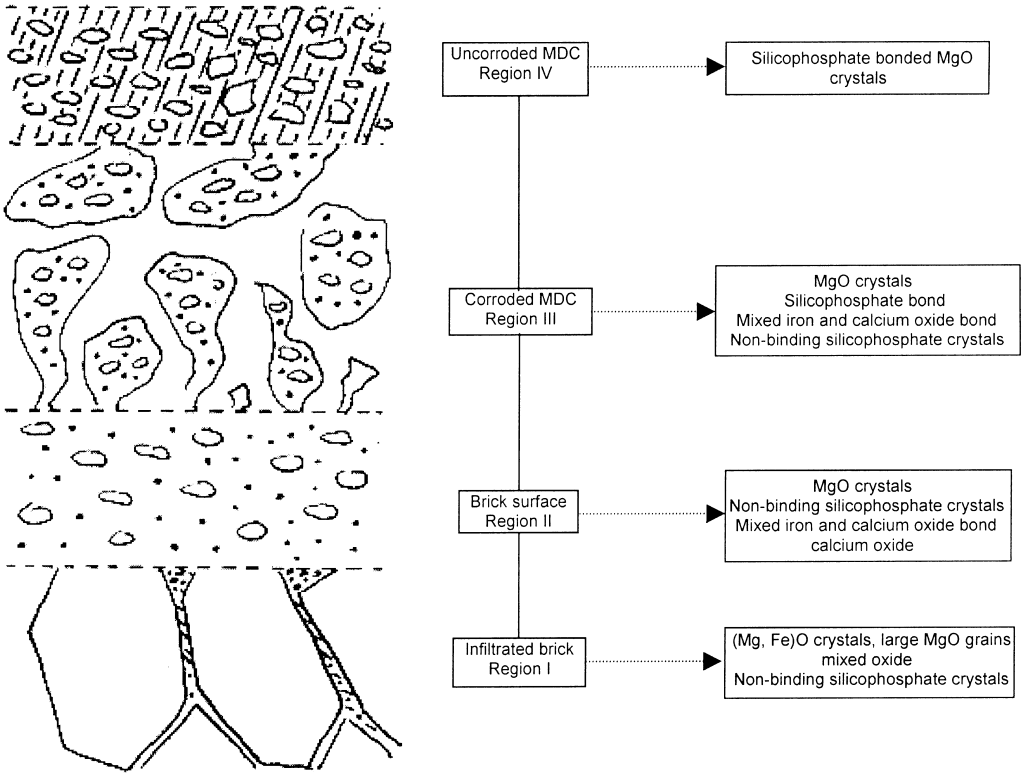

Fig. 7. Schematic profile of MgO-C/slag/MDC interface.

At interface (region II), the slag interaction with bricks has led to a dense layer which from the large periclase grains have disappeared. In this zone, MgO single crystals and silicophosphate crystals are embedded in a mixed calcium iron oxide. CaO forms a heterogeneously distributed phase.

In opposite to region II, the slag/MDC material interface (region III) exhibits a porous microstructure. In this section a (silico)phosphate phase coexists with the calcium iron oxide as a matrix. The matrix surrounds MgO and silicophosphate crystals. The porosity could explain the weakness of interface previously reported by G. Boiché et al.[4,15] No dolomite grains could be evidenced in MDC material, even at hot face of the investigated layers.

3.3.3. The interaction mechanism between slag and MDC

Investigations of the two main slag phases (calcium iron oxide and calcium silicate crystals) composition were carried out, by means of EDS analyses, along the cross section, in order to determine the interaction mechanisms at interface. The results are reported Figs. 8 and 9.

The iron calcium oxide contains some aluminium which proportion increases from 2.7 to 7.9% as slag penetrates the gunning material. The $\frac{Ca}{Fe}$ ratio is constant and equivalent to about $\frac{5}{3}$ all over the sample (Fig. 8).

The silicophosphate crystals exhibit Na and P contents increasing from the bricks/slag interface to the slag/MDC material interface. The increasing proportions of Na and P are associated with decreasing Ca and Si proportions (Fig. 9). This is in opposite to the trend observed for the binding silicophosphate, in which the Na and P contents decrease from interface to hot face (Fig. 10).

According to the evolution of the slag phases composition, the slag interaction with MDC materials mainly involves a reaction with the dolomite and $(NaPO_3)_n$ contents. Slag reaction with dolomite saturates the calcium iron oxide with calcium and rises its aluminium content. This increases the slag melting point and viscosity. In slag, CaO reacts with SiO_2 leading to the formation of Ca_2SiO_4 crystals. This reaction still occurs at interface with bricks. However, as slag capillary penetrates the gunned material, SiO_2 remaining in slag decreases. This yields the free CaO and SiO_2 to react with $(NaPO_3)_n$, brought by the MDC material, and form the refractory silicophosphate crystals embedded in the rich Na and P silicophosphate and calcium iron oxide matrix, observed at interface (region III). Although they are non-binding, the silicophosphate crystals resulting from this reaction increase the solid part of the bond which further improves viscosity and, therefore, adhesion of the gunned material to the slag-covered bricks. It is worth noting that the silicophosphate bond has formed, at interface, despite the lost in sodium and phosphorus elements resulting from their reaction with slag.

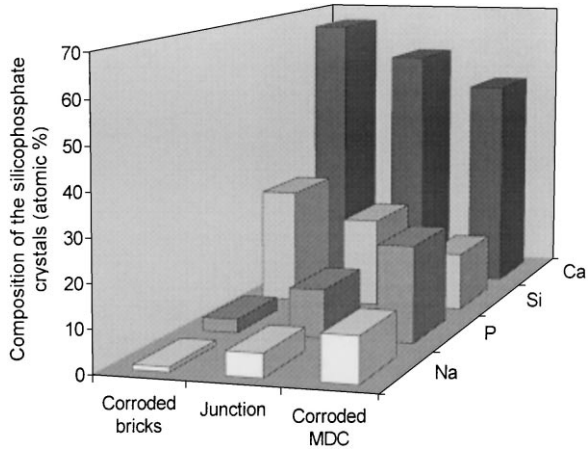

Fig. 9. EDS analyses of the non-binding silicophosphate crystals along the slag penetration front.

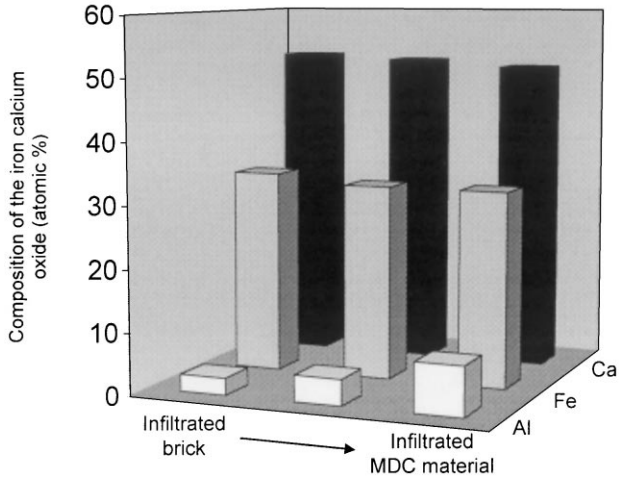

Fig. 8. EDS analyses of the calcium iron oxide in the slag infiltrated regions.

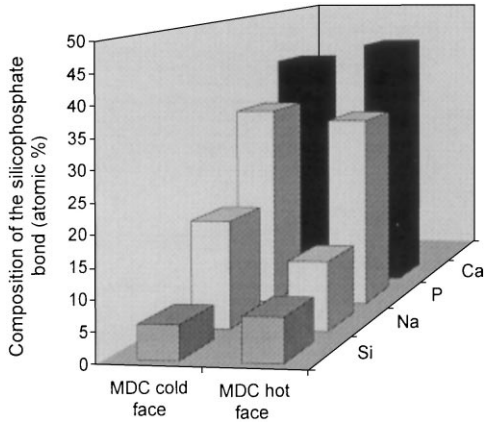

Fig. 10. EDS analyses of the silicophosphate bond in MDC material projected on slag covered MgO-C bricks.

4. Conclusion

According to the present work, the low corrosion resistance of olivine-containing materials is explained by the formation of low-melting point phases belonging to the $CaO–MgO–SiO_2$ system. Moreover, the Mg_2SiO_4 phase, contained in those samples, was found to react with the Ca, Si and Fe elements of slag, leading to solid solutions of $(Ca,Mg)MgSiO_4$ and $(Mg,Fe)_2SiO_4$ type. The forsterite enrichment in Fe decreases its melting point.

Slag interaction with dolomite-containing-materials involves low bulk modifications of the refractory material. This is due to a reaction between the slag elements and $(NaPO_3)_n$ and dolomite contents of the refractory material which increases the slag melting point via its enrichment in calcium and aluminium and the formation of refractory silicophosphate crystals. As a result, the slag penetration is limited. This protects the other refractory phases such as MgO. When slag is present, at interface of a gunned dolomite containing-material, the silicophosphate bond formation still occurs, however, the slag presence was also shown to result in large pores formation which could weaken the interface.

Acknowledgements

This work was supported by a Grant from the "Région Nord-Pas de Calais" and TRB manufacturer. We are grateful to Pr. J.B. Vogt from the "Laboratoire de Métallurgie" of the Université des Sciences et Technologie de Lille for allowing us to access to the Scanning Electron Microscope and Energy Dispersive Spectroscopy system and for fruitful discussions.

References

1. Siegl, W. M., Composition and application of basic refractory maintenance mixes. *Radex-Rundschau*, 1985, **4**, 706–723.
2. Yamanaka, H., Ikeda, M., Tamura, S. and Taira, H., Basic study on adhesion behavior of gunning material for BOF. *Taïbabutsu Overseas*, 1985, **5**(4), 35–42.
3. Ruchaud, N., Hubert, P., Rivenet, M., Abraham, F., Boivin, J. C., Pittini, G. and de Lorgeril, J., New gunning solutions for converters repairs at high temperatures. In *Proc. Unified International Technical Conference on Refractories*, UniteCR, 99, Berlin, Germany, 1999, pp. 161–164.
4. Boiché, G., *Contribution à l'Etude des Mécanisme d'Adhérence des Matériaux de Réparation des Convertisseurs d'Aciérie par Projection à Chaud*. CNAM thesis, Laboratoire de Chimie du Solide Minérale — Nancy I, France, 1980.
5. Rudolf, M. J., Steinmetz, P., Gleitzer, C., Guenard, C. and Adam, R., Etude de la réparation de revêtements de convertisseurs d'aciérie par projection de magnésie à travers une flamme. *Rev. Int. Hautes Tempér. Réfract. Fr*, 1983, **20**, 101–113.
6. Rivenet, M., Cousin, O., Boivin, J. C., Abraham, F., Ruchaud, N. and Hubert, P., A study of the $Na_2O–CaO–P_2O_5–SiO_2$ system in respect to the behaviour of phosphate bonded basic refractories at high temperature. *J. Eur. Ceram. Soc.*, 2000, **20**(8), 1169–1178.
7. Berthet, A. and Guenard, C., Contrôle des principaux paramètres de la réparation par projection des fours d'aciérie. *Rev. Métall.*, 1981, January, 1–13.
8. Yount, J. G., Hot gunning materials for basic oxygen furnace maintenance. *Am. Ceram. Soc. Bull.*, 1968, **47**(3), 259–263.
9. Andreasen, A. H. M. and Andersen, J., Über die beziehung zwischen kornabstufung und zwischenraum in produkten aus losen körnem (mit einigen experimenten). *Kolloid-Z*, 1930, **50**, 217–228.
10. Aliprandi, G., *Matériaux Réfractaires et Céramiques Techniques, Eléments de Céramurgie et de Technologie*. Septima, Paris, 1979 pp. 342–346.
11. Ando, J., Phase diagrams of $Ca_3(PO_4)_2–Mg_3(PO_4)_2$ and $Ca_3(PO_4)_2–NaCaPO_4$ systems. *Bull. Soc. Japan,* 1958, 1953, **31**, 201–205.
12. Levin, E. M., Robbins, U. R. and McMurdie, H. F., *Phases Diagrams for Ceramists*. The American Ceramic Society, Columbus OH. 1964, p. 210.
13. Levin, E. M., Robbins, U. R. and McMurdie, H. F., *Phases Diagrams for Ceramists*. The American Ceramic Society, Columbus OH. 1964, p. 236.
14. Eguchi, T., Ichiyama, H., Yoshimura, T., Kuroda, K. and Voga, M., Properties of CaO rich gunning material for converter. *Taïhabutsu Overseas*, 1991, **11**(2), 44–46.
15. Boiché, G., Steinmetz, P., Gleitzer, C. and Guenard, G., Etude des mécanismes d'adhérence des matériaux de réparation des convertisseurs d'aciérie par projection à chaud. *Rev. Int. Hautes Tempér. Réfract. Fr.*, 1980, **17**, 339–349.
16. Johnson, B., Recent developments in basic gunning refractories. *Proc. Electri. Furn. Conf.*, 1967, 87–88.
17. Rivenet, M., Boivin, J. C., Abraham, F., Ruchaud, N. and Hubert, P., β-$NaCaPO_4$ and $Ca_5(PO_4)_3OH$: low temperature forms of a silicophosphate bond precursor. *Phos. Res. Bull.*, 1999, **10**, 268–273.